Journal of Magnetic Resonance 214 (2012) 119–123

Contents lists available at SciVerse ScienceDirect

Journal of Magnetic Resonance

journal homepage: www.elsevier.com/locate/jmr

Direct EPR irradiation of a sample using a quartz oscillator operating at 250 MHz for EPR measurements

Hidekatsu Yokoyama *

Department of Pharmaceutical Science, International University of Health and Welfare, 2600-1 Kitakanemaru, Otawara 324-8501, Japan

ARTICLE INFO

Article history:
Received 17 August 2011
Revised 14 October 2011
Available online 30 October 2011

Keywords:
Loop-gap resonator
Quartz oscillator
Frequency shift coil

ABSTRACT

Direct irradiation of a sample using a quartz oscillator operating at 250 MHz was performed for EPR measurements. Because a quartz oscillator is a frequency fixed oscillator, the operating frequency of an EPR resonator (loop-gap type) was tuned to that of the quartz oscillator by using a single-turn coil with a varactor diode attached (frequency shift coil). Because the frequency shift coil was mobile, the distance between the EPR resonator and the coil could be changed. Coarse control of the resonant frequency was achieved by changing this distance mechanically, while fine frequency control was implemented by changing the capacitance of the varactor electrically. In this condition, EPR measurements of a phantom (comprised of agar with a nitroxide radical and physiological saline solution) were made. To compare the presented method with a conventional method, the EPR measurements were also done by using a synthesizer at the same EPR frequency. In the conventional method, the noise level increased at high irradiation power. Because such an increase in the noise was not observed in the presented method, high sensitivity was obtained at high irradiation power.

1. Introduction

Noise in an RF source is considered to be one of the sources of noise that prevent an increase in EPR sensitivity [1,2]. If a fixed frequency oscillator such as a quartz oscillator, whose noise level is lower than that of a wide frequency band oscillator such as a synthesizer, can be used directly as an RF source for an *in vivo* EPR spectrometer, its sensitivity may be enhanced. For this purpose, the resonant frequency of an EPR resonator must be tuned to the operating frequency of a quartz oscillator. I have already developed a frequency shift coil which can shift the resonant frequency of a loop-gap resonator (LGR) [3]. An LGR [4–6] is an EPR resonator that has been frequently used in *in vivo* studies [7–10]. In this study, EPR measurements were conducted using a quartz oscillator as an RF source and an LGR equipped with a frequency shift coil.

2. Experimental

2.1. RF source

A quartz oscillator operating at 250 MHz (AS25000SAA, AnaSem, Japan; frequency stability, 500 ppm) was used as the RF source. Because its output was rectangular wave, a sine curve was obtained by low-pass filtering (SLP-300, Mini Circuit, New York, NY; frequency range, DC-270 MHz) after DC elimination. A sample in an EPR resonator was directly irradiated at the output frequency of the quartz oscillator via a power amplifier (ZFL-2HAD, Mini Circuit; frequency range, 50–1000 MHz; gain, 11 dB). The SSB phase noise of the quartz oscillator at the posterior stage of the power amplifier was estimated to be -117 ± 3 dBc/Hz (at 100 kHz offset) based on the peak power and 100 kHz-offset power obtained by a spectrum analyser (FSEA, Rohde & Schwarz, Germany; frequency range, 9 kHz–3.5 GHz). This value was almost the same level for a synthesizer (MG3633A, Anritsu, Japan; frequency range, 10 kHz–2.7 GHz), which was used conventionally as an RF source for *in vivo* EPR spectrometer [1–3,10] (Fig. 1).

While the high frequency components (2nd and 3rd harmonics) were observed at the output of the quartz oscillator without the low-pass filter, they disappeared after low-pass filtering. No differences in the 100 kHz-offset power with or without the low-pass filter were observed (each value is -70 ± 2 dBm).

The EPR measurement method using the quartz oscillator or the synthesizer as an RF source is referred here as a Qz or conventional method, respectively. In both methods, the resonant frequency of the LGR was set at the same frequency.

2.2. LGR and frequency shift coils

The LGR used in this study was a one-gap type, with an electric shield (bridge shield; width, 10 mm; length, 20 mm) located inside

* Fax: +81 287 24 3521.
E-mail address: yokohide@iuhw.ac.jp

1090-7807/$ - see front matter © 2011 Elsevier Inc. All rights reserved.
doi:10.1016/j.jmr.2011.10.013

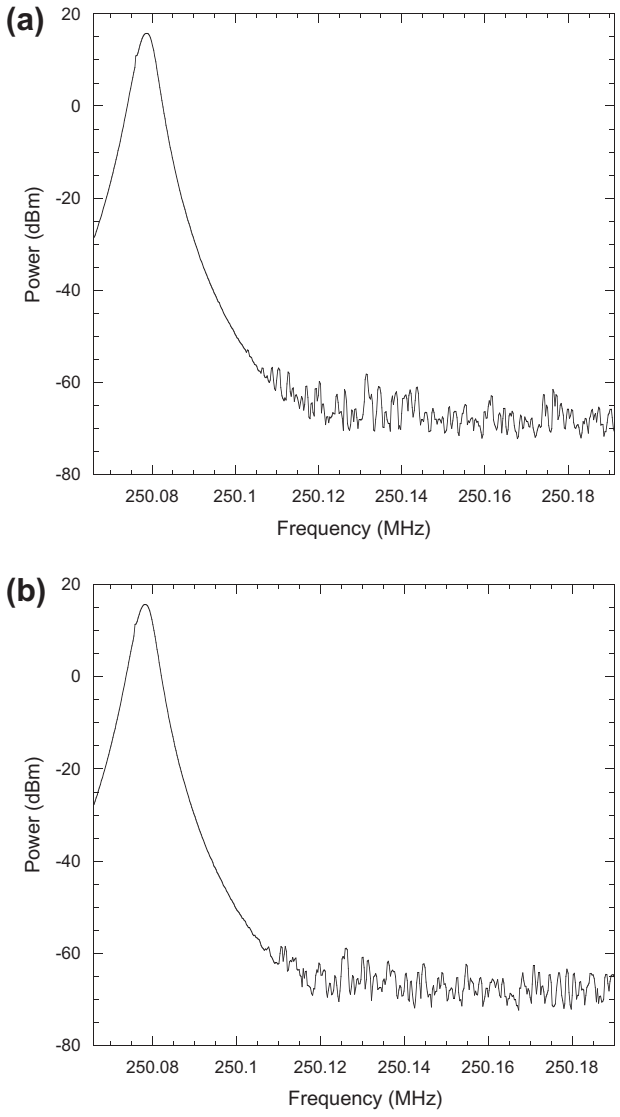

Fig. 1. Frequency characteristics of the RF source by the conventional (a) and Qz method (b). The measurement conditions were: frequency span, 125 kHz; resolution bandwidth, 3 kHz; sweep time, 50 ms. SSB phase noise (dBc/Hz) = [100 kHz − offset power] − [peak power] − 10 log(1.2·[resolution bandwidth]) + 2.5.

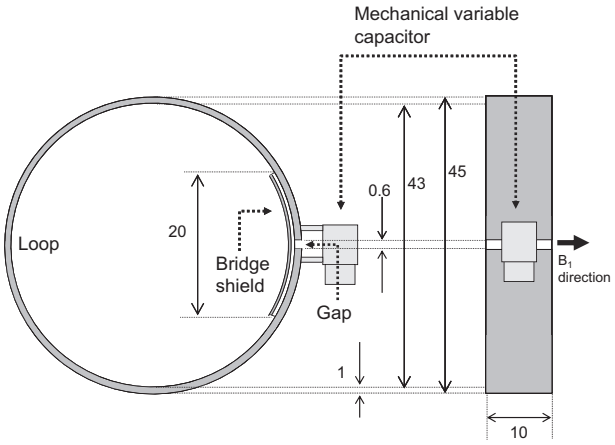

Fig. 2. Overview of the LGR. Dimensions are in mm. The bridge shield was located at the gap via a Teflon spacer that was 0.5 mm in thickness.

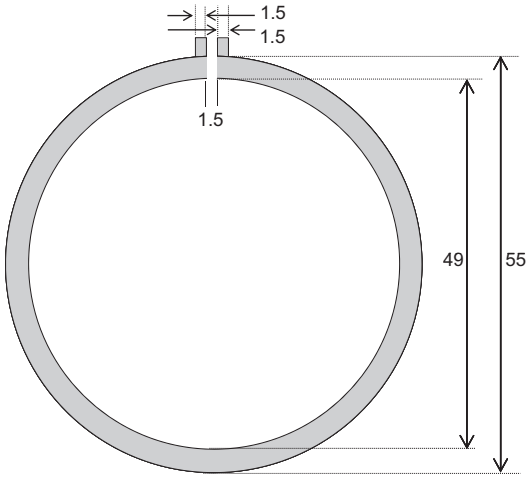

Fig. 3. Overview of the inductor of the frequency shift coil. Dimensions are in mm. The frequency shift coil was constructed from a single-turn coil of copper plate of thickness 0.1 mm. The copper plate was fixed on the ring-shaped acrylic plate of thickness 5 mm.

the resonator. The LGR dimensions were an inner loop diameter of 43 mm and an axial length of 10 mm. A loop of this size can accommodate the head of a rat or the whole body of a mouse [7–10]. In the gap, a mechanical variable capacitor (air trimmer capacitor, JMC5756, TOCOS, Japan; range, 0.6–6 pF) was connected in parallel (Fig. 2). The inductance of the loop of this LGR was calculated to be ca. 70 nH based on the loop size. The capacitance of the LGR which had been previously fabricated for a 700 MHz-EPR spectrometer [7–10] was calculated to be ca. 0.75 pF, based on the resonant frequency and the loop size. The sizes of the bridge shield and the loop of the 700 MHz-LGR were the same as those in this study. The 700 MHz-LGR was a two-gap type and had two bridge shields located inside the gap. Thus, the capacitance of one bridge shield in this study was estimated to be ca. 1.5 pF.

To operate the LGR in this study at a resonant frequency of 250 MHz, a capacitance of ca. 6 pF is required. Thus, the LGR can be operated near this frequency by adjusting the mechanical variable capacitor (range, 0.6–6 pF). RF power was supplied to the LGR via a coupling coil (a single-turn coil; diameter, 45 mm). The distance between the coupling coil and the LGR was adjusted to match their impedances.

A frequency shift coil was constructed from a single-turn coil (inner diameter, 49 mm; outer diameter, 55 mm) of copper plate of thickness 0.1 mm (Fig. 3). A fixed capacitor (3 pF; C_1 in Fig. 4) and a varactor diode (3–15 pF; 1SV153, Toshiba, Japan; D in Fig. 4) were serially connected to the terminal of the single-turn coil, which was located on the opposite side of the LGR to the coupling coil.

The resonant frequency of the frequency shift coil was calculated to be ca. 80 MHz based on the capacitances of the fixed capacitor and the varactor diode and the size of the coil. Because this value is sufficiently smaller than the operating frequency of the EPR resonator (250 MHz), the frequency shift coil functions as a shorted ring at 250 MHz.

When an inductor is located near a resonator with both magnetic fields aligned in the same direction, the inductance in the resonator is reduced due to mutual inductance. As a result, the resonant frequency of the resonator increases. Based on this phenomenon, the frequency shift coil can shift the operating frequency of the LGR [3]. Because the frequency shift coil was mobile, the distance between the LGR and the coil could be changed. Coarse

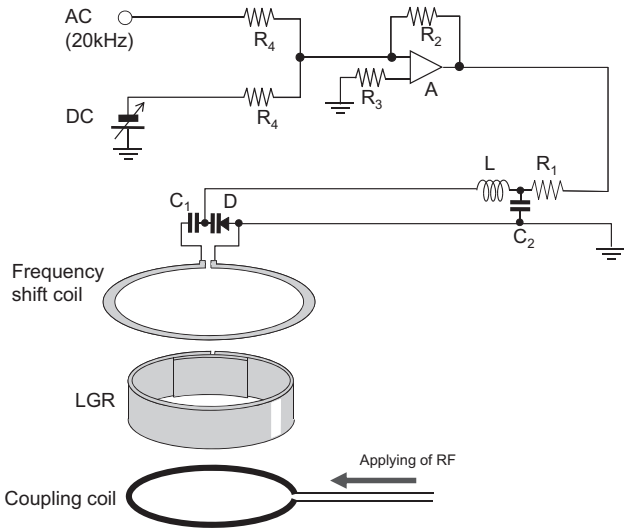

Fig. 4. Schematic diagram of the LGR and the frequency shift coil. A varactor diode (D) in series with a fixed capacitor (C_1) is connected to the single-turn coil. A reverse voltage is applied to the varactor diode by a bias voltage source via an inductor (L) and resistor (R_1). This resistor, together with a fixed capacitor (C_2), also serves as an RC circuit. To apply the FM to the frequency shift coil, a summing circuit of DC and AC (20 kHz), which consists of a stable unity gain and a high speed amplifier (A), is connected to the input of the frequency shift coil.

control of the LGR frequency was achieved by mechanically changing this distance, while fine frequency control was implemented by electrically changing the capacitance of the varactor.

The varactor diode, which has a capacitance that varies from 16.25 pF at a reverse voltage of 2 V to 2.43 pF at 25 V, is mainly used for electric tuning in the VHF and UHF bands [11]. The fixed capacitor prevents the DC from flowing into the single-turn coil when a DC reverse voltage is applied to the varactor diode. When the capacitance of the fixed capacitor is smaller than that of the varactor diode, most of the RF voltage is applied to the fixed capacitor, and the varactor diode contributes a smaller proportion of the total capacitance: thus it is a suitable means to provide fine control of the frequency.

A DC reverse voltage was applied to the varactor by a bias voltage source via an inductor (L in Fig. 4) and a resistor (R_1 in Fig. 4). The inductor (air core coil, 70 nH) and resistor (3.3 kΩ) prevent the leakage of the RF current. The resistance of the resistor is sufficiently large compared to the impedance of the varactor diode at the resonant frequency of the LGR. This resistor additionally serves as an RC circuit (time constant, 3.3 μs) with a fixed capacitor (1 nF; C_2 in Fig. 4), which protects the varactor from the voltage disturbance at a magnetic field modulation frequency of 100 kHz.

The resonator assembly was set at the center of a shield case, which prevents radiation from RF energy and noise penetration. The shield case is 70 mm wide, 145 mm deep, and 150 mm high. A pair of magnetic field modulation coils (inner diameter, 46 mm; outer diameter, 68 mm; number of turns, 40; separation between coils, 66 mm) was also located in this case. The *z*- and *x*-axes are defined as the directions of static (B_0) and RF (B_1) magnetic fields, respectively. The *y*-axis is perpendicular to the *z*–*x* plane. Because the width of the *x*-axis direction for flowing the eddy current caused by the magnetic field modulation in the frequency coil was very narrow (0.1 mm), this coil was barely influenced by the eddy currents.

FM is applied to the frequency shift coil and the RF phase is adjusted in homodyne detection such that the FM component in the reflection from an EPR resonator is minimized. The modulation frequency was set at 20 kHz so that the AC component of the FM could pass through the RC circuit in the frequency shift coil. The

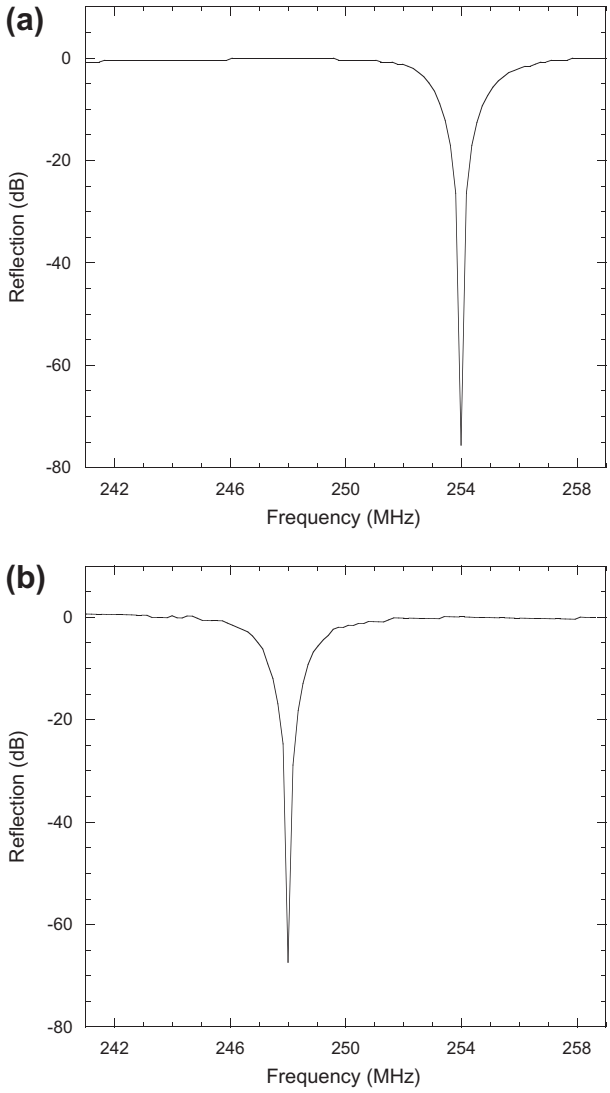

Fig. 5. Frequency characteristics of the LGR loaded with the phantom, under conditions of constant voltage applied to the varactor diode (0 V) and a distance between the LGR and frequency shift coil of 10 mm (a) or 15 mm (b).

summing circuit of DC and AC (20 kHz), which consisted of a stable unity gain and high speed amplifier (AD797, Analog Devices, Norwood, MA; A in Fig. 4), was connected to the input of the frequency shift coil.

2.3. EPR spectrometer

The RF EPR spectrometer used in this study has previously been described in detail [7–10]. Briefly, it consists of a main electromagnet, a pair of magnetic field sweep coils, a pair of magnetic field modulation coils, power supplies, a personal computer, an RF source for EPR excitation, RF circuits for homodyne detection, and intermediate-frequency circuits for lock-in detection at a magnetic field modulation frequency of 100 kHz. The width of the magnetic field modulation was set at 0.2 mT. The electromagnets were constructed at Yonezawa Electric Wire, and Yamagata Promotional Organization for Industrial Technology, Japan.

The RF source was connected to the RF circuits for homodyne detection which consisted of a directional coupler (ZFDC-10-5, Mini Circuit; frequency range, 1–2000 MHz; coupling coefficient, 10.8 dB; maximum input power, 0.5 W), a phase shifter (6602-3, Sage, Palo Alt, CA; frequency range, DC-2 GHz; minimum phase

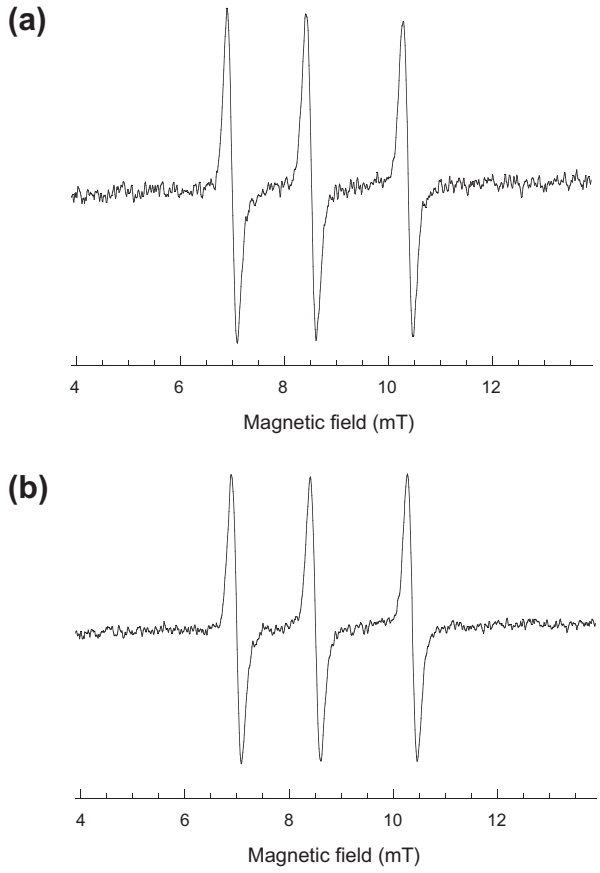

Fig. 6. Examples of the EPR spectra obtained by the conventional (a) and Qz method (b) at maximum incident power (50.6 or 46.7 mW). The EPR conditions were: EPR frequency, 250.078 MHz; static magnetic field, 8.9 mT; magnetic field sweep speed, 10 mT/s at a width of 10 mT; time constant, 1 ms; accumulation number, 2; magnetic field modulation, 0.2 mT at 100 kHz.

shift, 290 °/GHz), a variable attenuator (8494A, Agilent Technology, Palo Alt, CA; frequency range, DC-4000 MHz; maximum attenuation, 11 dB), a power amplifier (ZHL-2-12, Mini Circuit, frequency range, 10–1200 MHz; gain, 24 dB), a VSWR bridge (BR-1 N, Kuranishi, Japan; frequency range, 10–1300 MHz; insertion loss, 8 dB; maximum input power, 1 W), a preamplifier (ZFL-1000LN, Mini Circuit; frequency range, 0.1–1000 MHz; gain, 20 dB), and a double-balanced mixer (M49, R&K, Japan; frequency range, 1–2000 MHz).

2.4. Samples

A cylindrical phantom (diameter, 25 mm; axial length, 31 mm) was used to assess the performance of the system. The phantom consisted of agar containing 1 mM 4-hydroxy-2,2,6,6-tetramethylpiperidin-1-oxyl (TEMPOL; Aldrich Chemical Co., Milwaukee, WI), a nitroxide radical, and a physiological saline solution (a 0.9% aqueous sodium chloride solution). The phantom was placed at the center of the LGR.

3. Results and discussion

3.1. Frequency control using a frequency shift coil

The resonant frequency of the LGR loaded by the phantom was determined using a network analyzer (R3762B, Advantest, Japan; frequency range, 0.3–3600 MHz). The mechanical variable capaci-

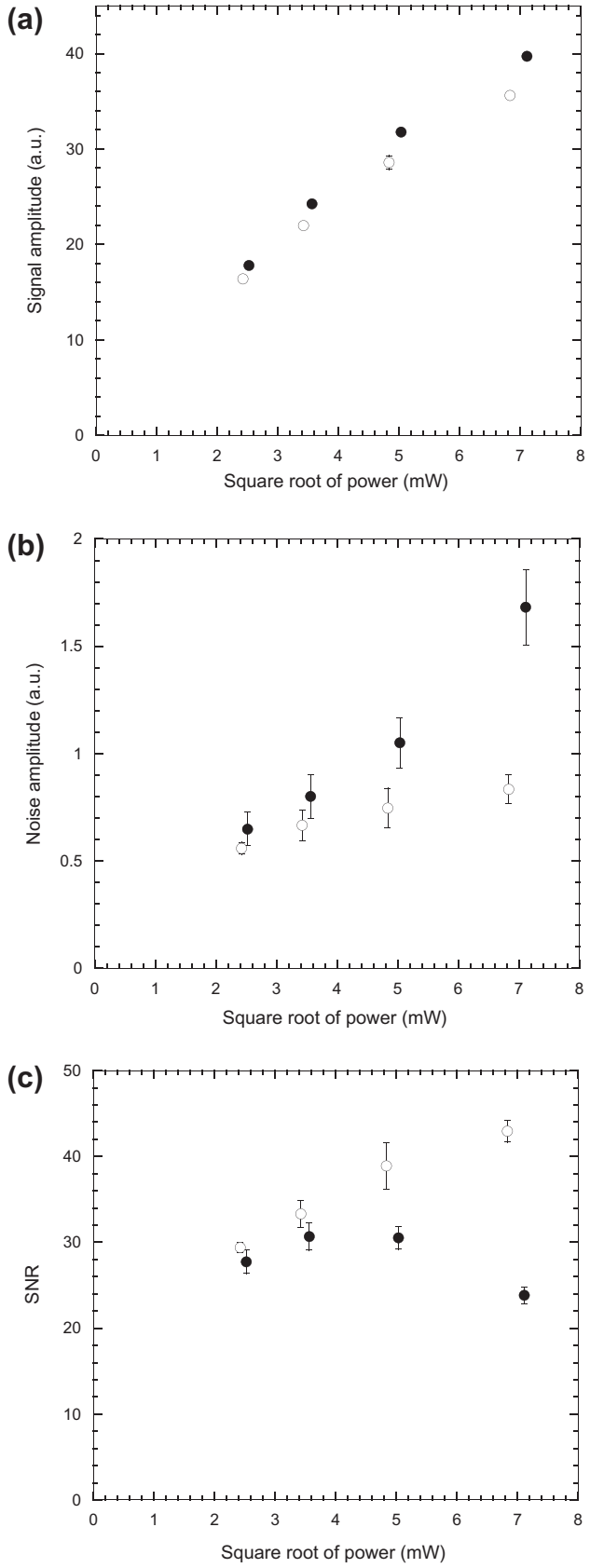

Fig. 7. The signal amplitude (a), noise amplitude (b), and SNR (c) of the conventional (closed circles) and Qz (open circles) methods versus the square root of the incident power. Values are mean ± standard error from 5 independent determinations.

tor on the LGR was adjusted so that the LGR without the frequency shift coil resonated at 248 MHz. The unloaded or loaded Q was 600 or 250, respectively.

When the distance between the LGR and the frequency shift coil was changed from 22 to 12 mm while maintaining a constant voltage to the varactor diode (0 V), a change in resonant frequency from 248 to 254 MHz was observed (Fig. 5). When the voltage to the varactor diode was changed from 0 to 15 V while maintaining a constant distance between the LGR and the frequency shift coil (12 mm), a shift of ca. 100 kHz was observed in the resonant frequency of the LGR.

3.2. EPR sensitivity at variable incident power

The EPR measurements of the phantom at variable incident power were made by both conventional and Qz methods. By using the frequency shift coil, the resonant frequency of the LGR with the phantom was tuned at the operating frequency of the quartz oscillator (250.078 MHz). B_1 at the sample per square root watt incident power is estimated to be ca. 45 μT, based on the size and loaded Q of the LGR. Examples of the EPR spectra obtained using both methods at the maximum incident power are shown in Fig. 6.

To achieve the FM at 20 kHz, the cutoff frequency of the RC circuit (R_1 and C_2 in Fig. 4) connected to the frequency shift coil was set at 48 kHz. A remarkable offset of the baseline in the EPR spectrum was not observed. This finding suggests that 100 kHz-magnetic field modulation barely affects the varactor connected to the frequency shift coil.

The signal amplitude was obtained from the peak-to-peak height of the lowest component in the triplet spectrum. The noise amplitude was defined as the product of the standard deviation (i.e., rms) from the baseline of the spectrum multiplied by $2\sqrt{2}$. The EPR sensitivity was estimated on the basis of the signal-to-noise ratio (SNR). The signal amplitudes, noise amplitude, and SNR versus square root of the incident power obtained by both methods are summarized in Fig. 7a–c.

The relationship between the EPR signal amplitude and the square root of the incident power was almost linear in both the conventional and the Qz method. At the maximum power, this relationship deviated slightly from linearity (Fig. 7a). While the noise level increased in proportion to the square root of the incident power in the conventional method (Fig. 7b, closed circles), its increase was relatively small in the Qz method (Fig. 6b, open circles). In the conventional method, the increase in the SNR with the increase in the incident power was not observed but rather the SNR decreased at high incident power (Fig. 7c, closed circles). On the other hand, the SNR of the Qz method increased with the increase in the incident power (Fig. 7c, open circles). The SNR in the Qz method at maximum power was twice that of the conventional method.

For converting the rectangular wave outputs of the quartz oscillator to sine waves, the low-pass filter was used in this study. When the same low-pass filter was connected to the output of the synthesizer, no remarkable reduction in the noise amplitude was observed.

At higher incident power, the sensitivity in the Qz method was greater than that in the conventional method. In the conventional method, an increase in the noise level was observed at higher incident powers. The RF source noise such as phase noise may be one of its origins [1,2]. Thus, it is thought that the RF source noise in the Qz method is smaller than that in the conventional method.

The values of the SSB phase noise estimated by using the spectrum analyzer were almost the same between the conventional and Qz method. The power at the 100 kHz offset of the RF source was −67 ± 2 dBm or −68 ± 3 dBm in the conventional or Qz method, respectively (Fig. 1). Each value changed to −71 ± 1 dBm when the power supply to the RF sources was turned off. The values of the 100 kHz offset observed by the spectrum analyzer were close to the noise level of the analyzer itself within one standard deviation. Thus, these would not reflect the appropriate noise level of the RF sources. Because the higher noise amplitude at a higher incident power was observed in the conventional method, it is thought that the phase noise from the RF source resulted in a lower SNR in this method. The differences in the phase noise between two methods might be levels that could not be detected by the spectrum analyzer.

4. Conclusion

In this study, direct EPR irradiation of a sample in an EPR resonator (loop-gap type) using a quartz oscillator operating at 250 MHz was performed to improve EPR sensitivity. Because the noise level of a fixed frequency oscillator such as a quartz oscillator is lower than that of a wide frequency band oscillator such as a synthesizer, the use of a quartz oscillator as an RF source for an *in vivo* EPR spectrometer for direct EPR irradiation may achieve an enhancement of sensitivity. To tune the operating frequency of the EPR resonator to that of the quartz oscillator, a single-turn coil with an attached varactor diode (frequency shift coil) was used. By using this apparatus and the quartz oscillator, high sensitivity EPR measurements of a phantom could be performed at high irradiation power.

References

[1] T. Sato, H. Yokoyama, H. Ohya, H. Kamada, An active resonator system for CW-ESR measurement operating at 700 MHz, J. Magn. Reson. 159 (2002) 161–166.
[2] H. Yokoyama, T. Sato, Development of surface-coil-type resonators consisting of an irradiation and receiver coil system for EPR measurements at 700 MHz, Appl. Magn. Reson. 29 (2005) 717–728.
[3] H. Yokoyama, Coarse and fine control of the EPR frequency of a loop-gap resonator using a single-turn coil with a varactor diode attached, Appl. Magn. Reson. 36 (2009) 49–59.
[4] W. Froncisz, J.S. Hyde, The loop-gap resonator: a new microwave lumped circuit ESR sample structure, J. Magn. Reson. 47 (1982) 515–521.
[5] M. Ono, T. Ogata, K. Hsieh, M. Suzuki, E. Yoshida, H. Kamada, L-band ESR spectrometer using a loop-gap resonator for in vivo analysis, Chem. Lett. (1986) 491–494.
[6] H. Hirata, M. Ono, Resonance frequency estimation of a bridged loop-gap resonator used for magnetic resonance measurements, Rev. Sci. Instrum. 67 (1996) 73–78.
[7] H. Yokoyama, S. Fujii, T. Yoshimura, H. Ohya-Nishiguchi, H. Kamada, In vivo ESR-CT imaging of the liver in mice receiving subcutaneous injection of nitric oxide-bound iron complex, Magn. Reson. Imaging 15 (1997) 249–253.
[8] H. Yokoyama, Y. Lin, O. Itoh, Y. Ueda, A. Nakajima, T. Ogata, T. Sato, H. Ohya-Nishiguchi, H. Kamada, EPR imaging for in vivo analysis of the half-life of a nitroxide radical in the hippocampus and cerebral cortex of rats after epileptic seizures, Free Radical. Bio. Med. 27 (1999) 442–448.
[9] H. Yokoyama, S. Morinobu, Y. Ueda, EPR imaging to estimate the in vivo intracerebral reducing ability in adolescent rats subjected to neonatal isolation, J. Magn. Reson. Imaging 23 (2006) 637–640.
[10] H. Yokoyama, T. Sato, T. Ogata, H. Ohya, H. Kamada, Automatic coupling control of a loop-gap resonator by a variable capacitor attached coupling coil for EPR measurements at 650 MHz, J. Magn. Reson. 149 (2001) 29–35.
[11] The Diode Manual, CQ Shuppan, Tokyo, 1995, pp. 192.